Catalytic conversions of chloroolefines over iron oxide nanoparticles
3.* Electronic and magnetic properties of γ-Fe_2O_3 nanoparticles immobilized on different silicas

T. N. Rostovshchikova,[a] O. I. Kiseleva,[a] V. V. Smirnov,[a] Yu. V. Maksimov,[b] I. P. Suzdalev,[b] V. E. Prusakov,[b] M. V. Tsodikov,[c] and V. N. Ikorskii[d]*

[a]Department of Chemistry, M. V. Lomonosov Moscow State University, 1 Leninskie Gory, 119992 Moscow, Russian Federation. Fax: +7 (495) 932 8846. E-mail: rtn@kinet.chem.msu.ru
[b]N. N. Semenov Institute of Chemical Physics, Russian Academy of Sciences, 4 ul. Kosygina, 119991 Moscow, Russian Federation. Fax: +7 (495) 137 8318. E-mail: maksimov@chph.ras.ru
[c]A. V. Topchiev Institute of Petrochemical Synthesis, Russian Academy of Sciences, 29 Leninsky prosp., 119991 Moscow, Russian Federation. Fax: +7 (495) 230 2224. E-mail: tsodikov@ips.ac.ru
[d]International Tomography Center, Siberian Branch of the Russian Academy of Sciences, 3a ul. Institutskaya, 630090 Novosibirsk, Russian Federation. Fax: +7 (383 2) 33 1399. E-mail: ikor@tomo.nsk.ru

Catalytic properties of superparamagnetic γ-ferric oxide nanoclusters, which are uniform in terms of size and magnetic properties were studied. The catalysts were supported on the activated silica gel matrix (AGM) prepared from the KSK-2 silica gel of globular structure and on the activated silica matrix (ASM) prepared from layered natural vermiculite. The clusters are active in some reactions of chloroolefin conversions: isomerization of dichlorobutenes and alkylation of benzene with allyl chloride. Their activity in these reactions is many times higher that of usual supported catalysts based on α-ferric oxide. Analysis of the Mössbauer spectra of the 2.5 wt.% Fe/AGM and 2.5 wt.%Fe/ASM samples before and after the reaction at T = 3—300 K shows that during the reaction some Fe^{III} ions arranged in ~2—3-nm γ-Fe_2O_3 nanoclusters magnetically ordered at 6 K are reduced to form a high-spin Fe^{II} complex in the paramagnetic state. According to the macroscopic magnetization data (SQUID) of the initial clusters, curves with hysteresis are observed at 2 K in the plots of forward and backward magnetization, while the 2.5 wt.%Fe/ASM catalyst after the reaction at T = 2 K demonstrates a linear field dependence of the magnetization passing through the coordinate origin. Analysis of the Mössbauer spectra and magnetic properties suggests that during the catalytic reaction the Fe^{III} ions in the γ-Fe_2O_3 nanoclusters interact with chloroolefin with the allylic structure to be partially reduced to the Fe^{II} ions that are bound in a complex containing chloride ions and O^{II} ion(s) of the silicate matrix as ligands. This is a reason, probably, for the high catalytic activity of γ-Fe_2O_3 nanoparticles.

Key words: chloroolefins, isomerization, alkylation, γ-ferric oxide nanoclusters, silicas, iron(II) oxychloride, Mössbauer spectroscopy, magnetic properties, hysteresis loop.

Supported nanosized iron oxide clusters with superparamagnetic properties are of interest as catalysts of a new generation. We have previously[1—4] found that superparamagnetic nonstoichiometric nanoclusters γ-Fe_2O_{3-x} ($0 < x < 1/3$) with $d \approx 2$—3 nm prepared from iron(III) acetylacetonate and stabilized on activated mesoporous silica gel (AGM) or on the activated layered silica matrix (ASM) exhibit high activity in catalytic conversions of chloroolefins. This was assumed to relate to the formation of mixed-valence iron oxides favored by specific conditions or by the action of chloroolefins.[1—3] The role of structures including two charge states of iron ions (Fe^{II} and Fe^{III}) was also found in the Fischer—Tropsch reaction and some other catalytic processes.[5,6]

The purpose of the present work is to compare the catalytic activity of γ-Fe_2O_{3-x} nanoparticles prepared by the impregnation of the AGM and ASM with iron(III) acetylacetonate (2.5 wt.%) followed by thermolysis. The

* For Part 2, see Ref. 1.

Published in Russian in *Izvestiya Akademii Nauk. Seriya Khimicheskaya,* No. 10, pp. 1705—1711, October, 2006.
1066-5285/06/5510-1768

isomerization of 3,4-dichlorobut-1-ene (3,4-DCB) and benzene alkylation with allyl chloride were chosen as model reactions. In addition, it was of interest to reveal the nature of mixed-valence iron complexes formed on the supported catalysts upon the interaction with chloroolefin of allylic structure. Changes in the electronic and magnetic properties of the catalysts during the reactions were examined by Mössbauer spectroscopy in the temperature interval 3—80 K and using measurements of macroscopic magnetization (SQUID) in the range 2—300 K.

Experimental

Silica gel KSK-2 of usual globular structure and layered silica prepared from natural vermiculite[2,3] were used for supporting γ-ferric oxide. The initial crystalline vermiculite contained ~14 wt.% Al, 1 wt.% Ca, 2 wt.% Mg, and 1 wt.% Fe, as well as trace amounts of other metals. Vermiculite was subjected to two-step acid leaching in a mixture of hydrochloric and sulfuric acids followed by washing.[5] All metal ions were almost completely removed by the acid treatment, which was confirmed by elemental analysis. Activation resulted in substantial changes in the properties of layered silica: amorphization of the material, an increase in the specific surface area to 350 $m^2\,g^{-1}$, and an increase in the micropore fraction.[7] Iron (2.5 wt.%) was supported on the ASM samples obtained after activation. For this purpose, the activated matrix was impregnated with a solution of $Fe(acac)_3$ with a specified concentration followed by drying in air, evacuation, and heating at 400 °C. Temperature-programmed heating was carried out with a rate of 10 deg min^{-1}. Then the sample was stored for 2 h at 400 °C. The obtained catalyst 2.5 wt.% Fe/ASM (hereinafter 2.5% Fe/ASM) is amorphous to X-rays.

Iron was supported on mesoporous silica gel KSK-2 after preliminary activation of the silica gel by the single treatment with hydrochloric acid followed by washing. Iron (2.5 wt. %) was supported on the obtained AGM sample by impregnation with a solution of $Fe(acac)_3$. The AGM surface area was 340 $m^2\,g^{-1}$. The 2.5 wt.% Fe/AGM sample (hereinafter 2.5% Fe/AGM) is also amorphous to X-rays.

Isomerization of 3,4-DCB and alkylation of benzene with allyl chloride were conducted in sealed glass ampules with stirring in the temperature interval 70—110 °C in the presence of oxygen. Procedures of catalytic experiments, analysis of the composition of reaction mixtures by chromatography and GC-MS, and calculation of the catalytic activity have previously[2,3] been presented in detail. The major products of 3,4-DCB isomerization is *trans*-1,4-dichlorobut-2-ene. The yield of the *cis*-isomer does not exceed 2%. The reaction of benzene with allyl chloride affords mainly allylbenzene and 1-phenyl-2-chloropropane. Their ratio depends on the process conditions. Allylbenzene prevails at low conversions and then its ratio in the reaction mixture decreases, while that of 1-phenyl-2-chloropropane increases.[3] Particular experiments showed that 1-phenyl-2-chloropropane can be formed due to the catalytic hydrochlorination of allylbenzene. In both cases, at high conversions the reaction products contain up to several percentage of by-products, such as chloroprene, products of chloroolefin oligomerization and benzene translalkylation, and products of their oxidation including aldehydes and ketones of complicated structure. In the IR spectrum of allyl chloride (recorded on an In Fralum FT 801 FT-IR spectrophotometer in the 400—4000 cm^{-1} range) heated with the 2.5% Fe/ASM catalyst in a decane solution at 110 °C, the intensity of the absorption band of the C=C bond stretching vibration (1640 cm^{-1}) weakens and new absorption bands appear (1740, 1737, 1793, and 1797 cm^{-1}) that are characteristic of stretching vibrations of the carbonyl groups.[8]

Mössbauer spectra were obtained on a Wissel electrodynamic spectrometer with a source of ^{57}Co (Rh) γ-radiation (activity 10—20 mCi) in the temperature interval 3—80 K. Isomeric shifts were calculated relative to the center of magnetic HFS lines of α-Fe. The spectra were processed using standard least-square programs for the Mössbauer transition $3/2 \rightarrow 1/2$.

Magnetic properties of iron-containing samples were studied in the temperature interval 2—300 K on an SQUID magnetometer of the International Tomography Center (Siberian Branch of the Russian Academy of Sciences, Novosibirsk). To measure the static magnetic susceptibility, a sample was cooled in the zero magnetic field down to $T = 1$ K, then the measurements were conducted in the field with $H = 5000$ Oe with a temperature increment of 10—50 K in the interval from 2 to 300 K.

X-ray diffraction analysis of the iron-containing phases was carried out on a DRON-3M diffractometer using filtered Cu-Kα radiation.

Results and Discussion

Catalytic properties of γ-ferric oxide nanoparticles immobilized on silicas

Isomerization of 3,4-DCB. Isomerization of 3,4-DCB occurs quantitatively in the presence of γ-ferric oxide nanoparticles supported on silicas of the both types without an induction period at rather low temperatures (>70 °C). The catalytic activities of the two catalysts on the AGM and ASM supports are compared in Fig. 1. It is seen that at 70 and 80 °C the AGM-based catalyst excels in activity the ASM-based catalysts. However, their ac-

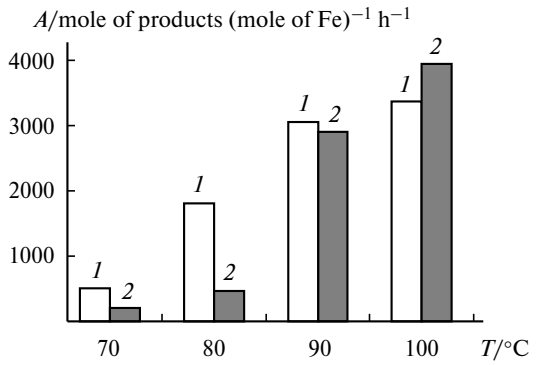

Fig. 1. Comparison of the catalytic activity of γ-Fe_2O_3 (*A*) on the AGM (*1*) and ASM (*2*) in the isomerization of 3,4-DCB at different temperatures.

tivities become comparable with the temperature increase to 90 °C, whereas at 100 °C the γ-Fe_2O_3 nanoparticles on the ASM are more active than those on the AGM. The maximum activity of the 2.5% Fe/ASM catalyst at 100 °C is more than an order of magnitude as high as the activity achieved for the most active catalyst based on α-Fe_2O_3 with a high (15%) Fe content.[2] The apparent activation energies calculated from the temperature plots of the rate constants of the forward and backward reactions were 65 and 78 kJ mol^{-1} for the AGM catalyst and 128 and 140 kJ mol^{-1} for the ASM-based samples. These values are higher than those found previously for larger iron oxide particles in similar catalytic systems.[1,2] The high apparent activation energies and a lower catalytic activity at moderate temperatures for the ASM are caused, probably, by the fact that at relatively low temperatures small γ-Fe_2O_3 clusters immobilized on the layered silica matrix are less accessible to the reactants that larger particles. The ASM support is a sorbent with the labile layered structure[9] in which the distance between the layers and, hence, a possibility of insertion into the interlayer space for molecules of organic reactants enhances with the temperature increase. Another possible explanation is associated with the strong interaction of the catalyst active phase with the layered silica matrix. It is most likely that the temperature increase facilitates transportation of a 3,4-DCB molecule to the active sites of the catalyst or weakens the interaction of the small iron oxide particles with the support. The catalysts retain high activity upon multiple (up to five cycles) utilization in catalysis.

Alkylation of benzene with allyl chloride. The catalytic properties of the γ-ferric oxide nanoparticles on the AGM and ASM in benzene alkylation with allyl chloride are comparable. Figure 2 shows the kinetic curves of allyl chloride consumption in the reaction with benzene to form two products, namely, allylbenzene and 1-phenyl-2-chloropropane,[3] at 110 °C for the catalysts under discussion. It can be seen that the initial reaction rate in the presence of the AGM-based catalyst slightly exceeds the process rate for the catalyst based on the ASM. The catalytic activities calculated from the initial rates were 144 and 117 moles of products (mole of Fe)$^{-1}$ h^{-1} for the AGM and ASM, respectively. However, the catalyst based on the AGM rapidly loses activity and the allyl chloride consumption ceases with time, whereas the ASM-based catalysts retain activity and can be used repeatedly (see Fig. 2).

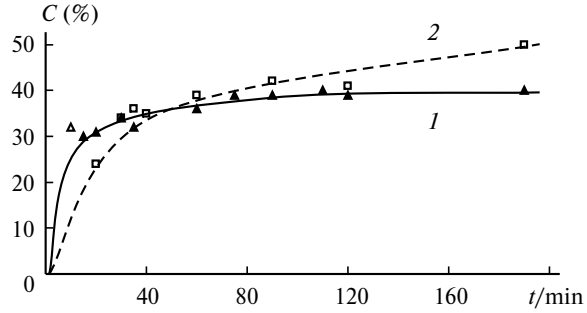

Fig. 2. Kinetic curves of accumulation of the products (*C*) of benzene (9.7 mol L^{-1}) alkylation with allyl chloride (2.5 mol L^{-1}) at 110 °C ([Fe] = 0.01 mol L^{-1}) in the presence of γ-Fe_2O_3 on the AGM (*1*) and ASM (*2*).

Both the isomerization of 3,4-DCB[2] and alkylation of benzene on the supported γ-ferric oxide nanoparticles occur without a noticeable induction period. These catalysts are almost 20 times as active as the most active analogs based on the α-Fe_2O_3 nanoparticles: for the latter the activity did not exceed 5—6 moles of allyl chloride (mole of Fe)$^{-1}$ h^{-1} even at a high iron content (12%).[3]

Mössbauer spectra and magnetic measurements

Catalyst evolution under the action of chloroolefins was studied in detail for 3,4-DCB isomerization, because the low boiling point of allyl chloride impeded experiments. At the qualitative level the changes in the Mössbauer spectra of the γ-Fe_2O_3 nanoparticles after heating with 3,4-DCB or with an allyl chloride—benzene mixture are close. The Mössbauer spectra of the 2.5% Fe/AGM catalyst before and after the catalytic isomerization of 3,4-DCB are shown in Fig. 3. The parameters of the spectra of the 2.5% Fe/AGM and 2.5% Fe/ASM samples obtained at 78 and 3 K are summarized in Table 1. The spectrum of the initial 2.5% Fe/AGM catalyst at 78 K contains only a "paramagnetic" doublet from the high-spin Fe^{III} complex in the octahedral environment of the O^{II} ions. The parameters of the spectrum of the complex differ substantially from those of the relaxation spectrum of $Fe(acac)_3$ used for iron supporting.[3] The spectrum at 6 K (see Fig. 3, *a*) is characterized by the magnetic HFS lines with H_{in} = 45.0 T and a "paramagnetic" doublet with a relative content of 22%. The observed transformation of the spectrum with the temperature change from 78 to 6 K is typical of the superparamagnetic system of γ-ferric oxide with the particle size $d \approx 2$—3 nm.[3]

The magnetic properties of the initial catalysts before testing in the reactions are rather close.[3,7] For the both samples, the runs of the magnetic susceptibility curves $\chi(T)$ are similar and the absolute χ curves almost coincide, which indicates magnetic homogeneity of the samples. The extrapolation of the rectilinear (high-temperature) regions of the curves to the low-temperature region showed that the χ^{-1}—T plots for the two catalysts obey the Curie—Weiss law with the negative values of the Weiss constants. This is typical of the superparamagnetic iron oxide clusters with the antiferromagnetic type of magnetic ordering. The χ^{-1}—T plot for the 2.5% Fe/ASM sample was characterized by a sharp decrease in the re-

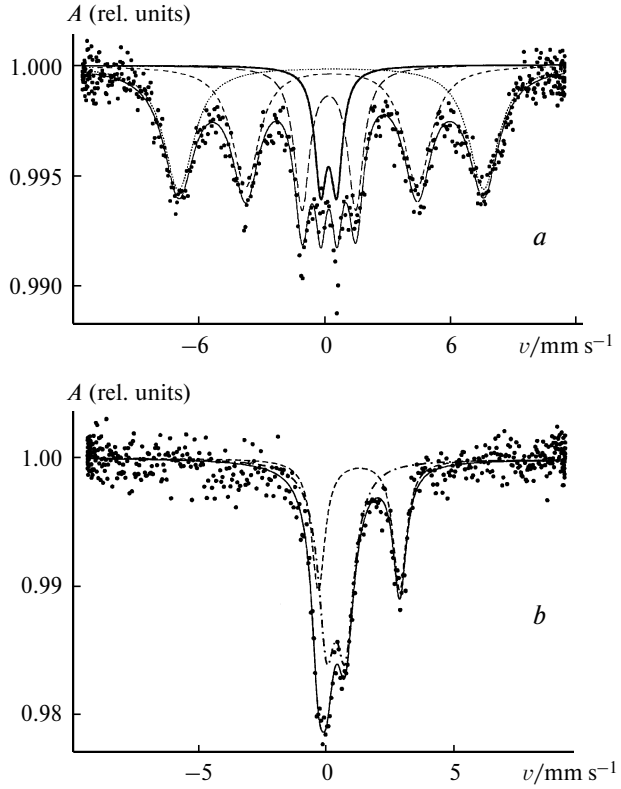

Fig. 3. Mössbauer ^{57}Fe spectra of the initial catalyst 2.5% Fe/AGM at 6 K (*a*) and the same catalyst after 3,4-DCB isomerization at 3 K (*b*) (υ is the rate of γ-radiation source).

gion ≤10 K, unlike the smooth decrease at ≤50 K for the 2.5% Fe/AGM system. The sharper decrease in the χ^{-1} values at $T \leq 10$ K indicates that for the ASM the cluster size distribution is more narrow than that for the AGM. The presence of the small γ-ferric oxide magnetic clusters in the 2.5% Fe/AGM and 2.5% Fe/ASM samples is confirmed by hysteresis loops in the curves of forward and backward magnetization of the samples at 2 K.[7]

The low-temperature Mössbauer spectra of the 2.5% Fe/AGM and 2.5% Fe/ASM catalysts after 3,4-DCB isomerization differ sharply from the low-temperature spectra of the initial samples. The spectrum of the 2.5% Fe/AGM sample recorded at 3 K after the reaction is presented in Fig. 3, *b*, and the spectral parameters of the same sample at 300 and 78 K (which are omitted in the figure) and at 3 K are given in Table 1. Note that the lines of magnetic HFS characterizing the magnetically ordered γ-Fe_2O_3 clusters, which were present in the sample before catalysis, disappear in samples used in catalysis. In addition, lines of the doublet from the octahedrally coordinated high-spin Fe^{II} complex with a relative content of 32 and 38%, respectively, appear in the spectra of the 2.5% Fe/AGM sample at 78 and 3 K along with the "paramagnetic" doublet from the octahedral high-spin complex of Fe^{3+} with a relative content of 68 and 62%, respectively.

Table 1. Parameters of the Mössbauer spectra for the 2.5% Fe/AGM catalysts before and after catalysis and for the 2.5% Fe/ASM catalyst after catalysis (δ is the isomeric shift relative to α-Fe, Δ is the quadrupole splitting or quadrupole shift, H_{in} is the internal field on the ^{57}Fe nucleus, and *A* is the relative content)

T /K	Component	δ±0.03	Δ±0.03	H_{in}±0.5 /T	*A*±5 (%)
		mm s^{-1}			
	2.5% Fe/AGM (before entry)[3]				
78	Fe^{3+}(paramagn.)	0.33	0.93	—	100
6	Fe^{3+}(paramagn.)	0.32	0.76	—	22
	Fe^{3+}(magn.)	0.29	0.00	45.0	78
	2.5% Fe/AGM (after entry)*				
300	Fe^{3+}(paramagn.)	0.32	0.62	—	78
	Fe^{2+}(paramagn.)	1.15	2.13	—	22
78	Fe^{3+}(paramagn.)	0.37	0.63	—	68
	Fe^{2+}(paramagn.)	1.24	3.02	—	32
3	Fe^{3+}(paramagn.)	0.38	0.73	—	62
	Fe^{2+}(paramagn.)	1.28	3.22	—	38
	2.5% Fe/ASM (after entry)*				
300	Fe^{3+}(paramagn.)	0.35	0.61	—	59
	Fe^{2+}(paramagn.)	1.14	2.11	—	41
78	Fe^{3+}(paramagn.)	0.37	0.47	—	69
	Fe^{2+}(paramagn.)	1.17	2.91	—	31

* Data of the present work.

The spectrum of the 2.5% Fe/ASM sample after catalysis obtained at 78 K resembles the corresponding spectrum of the 2.5% Fe/AGM catalyst. The spectrum contains lines only of the high-spin complexes of tri- and bivalent iron, whose parameters are given in Table 1. The macroscopic susceptibility data for the 2.5% Fe/ASM catalyst before and after 3,4-DCB isomerization are shown in Figs 4 and 5. It is seen that after the reaction the magnetization curve becomes smoother (see Fig. 4, *b*) and no hysteresis loop is observed contrary to the initial catalyst (see Fig. 4, *a*). This is especially noticeable in inset (see Fig. 4, *b*), where the linear magnetization isotherm at 2 K is presented.

The curves of the temperature dependence of the inverse magnetic susceptibility ($1/\chi$) of the 2.5% Fe/ASM catalyst (see Fig. 5, *a*, *b*) show that the plot of $1/\chi$ *vs.* *T* is linear for neither the initial sample nor the sample over which 3,4-DCB was isomerized. In the both cases, the extrapolation of the curves in the high-temperature region to low temperatures gives the intersection point at negative temperatures. As already observed above, this χ^{-1}—*T* dependence is characteristic of superparamagnetic clusters with the antiferromagnetic type of magnetic ordering.

Evidently, the structure of the γ-ferric oxide nanoclusters ($d \approx 2$—3 nm), which are present in the initial

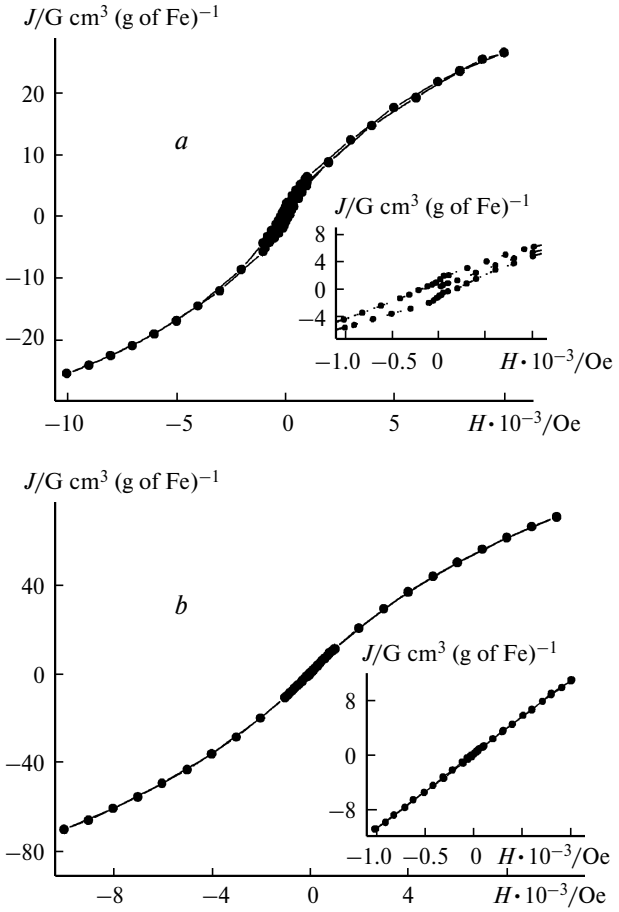

Fig. 4. Magnetization (J) isotherms of the 2.5% Fe/ASM sample before (*a*) and after catalysis (*b*) at 2 K. An expanded fragment of the J isotherm in the region -1000 Oe $\le H \le$ 1000 Oe is shown in insets.

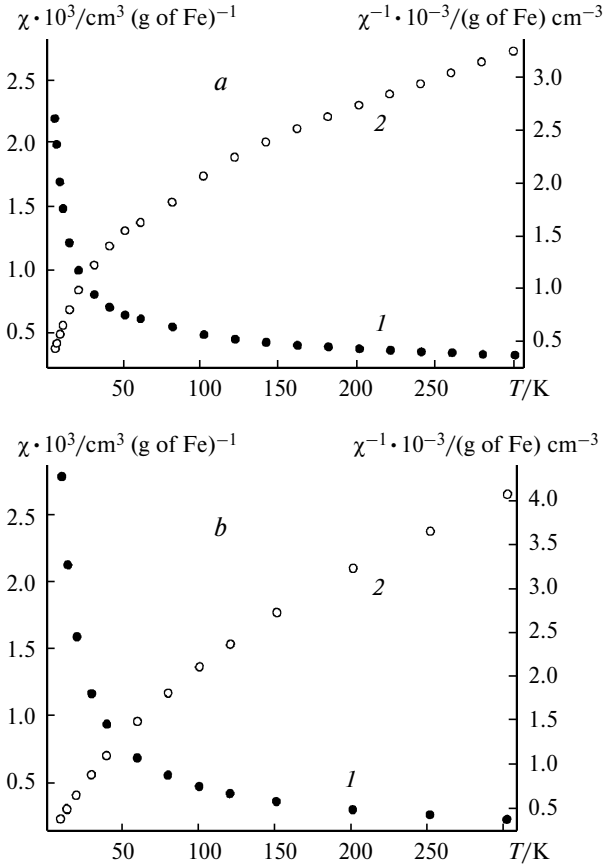

Fig. 5. Temperature plots of the magnetic susceptibility χ (*1*) and parameter $1/\chi$ (*2*) for the 2.5% Fe/ASM sample before (*a*) and after catalysis (*b*) (H = 5000 Oe).

state of the catalyst, undergo the substantial rearrangement under the action of chloroolefins. According to the Mössbauer spectroscopic data, some Fe^{III} ions are reduced to Fe^{II}, and the reduced ions exist in the paramagnetic state. The other Fe^{III} ions are not isolated and still participate in exchange interactions within the nanoclusters with sizes smaller than 2—3 nm. The absence of a hysteresis loop and the linear dependence of the curves of forward and backward magnetization (see Fig. 4, *b*) can be explained as follows. The cluster exists in the single-domain state until the cluster sizes achieve some critical value.[10] In the absence of domain boundaries, transmagnetization can occur through uniform (coherent) or nonuniform rotation of the spontaneous magnetization vector J.[11] According to the model of uniform rotation of the spontaneous magnetization vector in a magnetically uniaxial nanocrystal, the φ angle between the direction of the external magnetic field H and easy-magnetization axis is the parameter determining hysteresis.[11] The equilibrium orientation of J is determined by the ratio of the magnetic anisotropy energy (because of which J tends to be oriented along the easy-magnetization axis) and the magnetization energy of the magnetized sample in the magnetic field due to which J tends to be oriented along the H field. In the considered model, the hysteresis loop is transformed into a straight line at $\varphi = 90°$. In this case, magnetization in the positive and negative fields occurs through the reversible gradual rotation of J.

Let us consider the Mössbauer parameters of the Fe^{II} ion formed upon the interaction with chloroolefin. The parameters of the high-spin octahedral Fe^{II} complex formed in the reaction are analogous to the parameters of similar $FeCl_2$ complexes. The isomeric shifts (δ) of the Fe^{2+} complex obtained in the present work at 3—300 K range within ~1.13—1.30 mm s^{-1}, which corresponds to the data for compounds of the following series: $FeCl_2$, $FeCl_2 \cdot H_2O$, $FeCl_2 \cdot 2H_2O$, and $FeCl_2 \cdot 4H_2O$ ($\delta \approx$ 1.1 (300 K)—1.4 (5 K) mm s^{-1}).[12] More definite conclusions about the composition and electronic structure of the $FeCl_2$ complex formed in the reaction follow from analysis of the quadrupole splitting values (Δ). The Δ values for anhydrous $FeCl_2$ and three its crystal hydrates at different temperatures are compared in Fig. 6. Solid lines show the linear anamorphoses of the Δ values measured earlier[12—14]

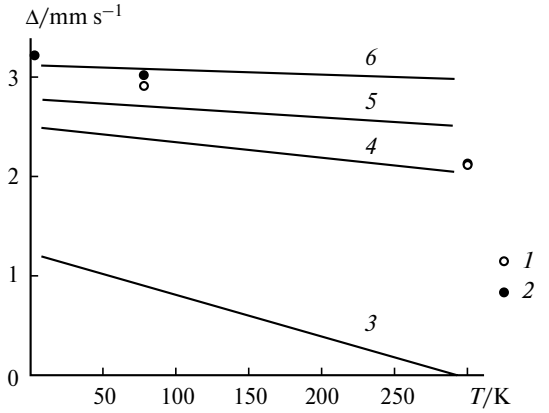

Fig. 6. Experimental (points) and literature data (lines) on quadrupole splitting of the Fe^{II} ion (Δ) in the temperature interval 3—300 K for the 2.5% Fe/AGM (*1*) and 2.5% Fe/ASM catalysts (*2*) after the reaction and for $FeCl_2$ (*3*), $FeCl_2 \cdot H_2O$ (*4*), $FeCl_2 \cdot 2H_2O$ (*5*), and $FeCl_2 \cdot 4H_2O$ (*6*).

in a wide temperature interval (0.15—300 K). It is seen that the quadrupole splitting values obtained in the present work correspond to hydrated $FeCl_2$ rather than anhydrous iron chloride. The increase in the Δ values on going from anhydrous $FeCl_2$ to the hydrated forms $FeCl_2 \cdot nH_2O$ is related to the fact that in the structure of the local polyhedron (octahedron) of Fe^{II} one, two, or four bridged chlorine ions are substituted for the corresponding number of oxygen ions from the water molecules.[12] Nonequivalence of the ligands results in an increase in crystalline field nonuniformity and an increase in quadrupole splitting.

The analysis performed agrees with the assumption on the formation of bivalent oxychloride upon the interaction of the catalyst with chloroolefin. The ability of iron oxides to perform dehydrochlorination of chlorohydrocarbons is well known.[15] In particular, the presence of a low amount of chloroprene in the products of 3,4-DCB isomerization is caused, most likely, by the dehydrochlorination of 3,4-DCB. In benzene alkylation with allyl chloride, the formation of allylbenzene is accompanied by the release of hydrogen chloride. The latter can also interact with the catalyst, for instance, replacing its hydroxyl groups by the chloride anion with water formation. In turn, chloroolefins undergo the whole series of transformations in the presence of iron oxides. Such a sequence of processes is possible when Fe^{III} is partially reduced to Fe^{II} by the oxidation of chloroolefin molecules (Scheme 1).

Olefin oxidation over the oxide catalysts is known to be promoted by chlorine-containing organic compounds.[16] Absorption bands of carbonyl groups were observed by IR spectroscopy in the spectra of allyl chloride after heating with the catalyst.

The appearance of Fe^{II} ions in the catalyst structure facilitates the C—Cl bond cleavage that occurs, probably,

Scheme 1

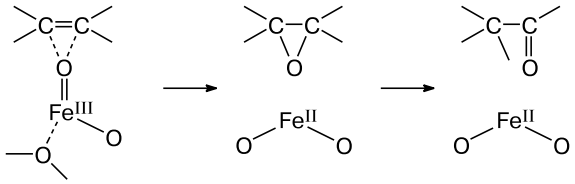

through the step of electron transfer from the catalyst to the reactant with the formation of the chloride anion.[1—4,15] The chloride anion is inserted into the structure of a complicated active site including iron ions in two oxidation states, as well as anionic and cationic vacancies and labile lattice oxygen,[2,3] and is involved in further steps of chloroolefin conversion.

From the data of the present work it is difficult to conclude about the amount and role of oxygen ions in the nearest environment of the Fe^{II} ion. When assuming that oxygen of the support lattice can be one of the polydentate ligands in the structure of the local Fe^{II} polyhedron, then the mechanism of strong cluster—support interaction is operative.

Note that $FeCl_2$ possesses no catalytic activity in conversions of chloroolefins.[4] However, the process is favored if the catalytically active site contains simultaneously the Fe^{III} and Fe^{II} ions and at least two types of ligands, *viz.*, chloride anion and oxygen-containing groups.

Since changes in the oxidation state of the iron ions and their ligand environment during the interaction with the reactants appear feasible, the absence of induction periods in chloroolefin conversions over the γ-ferric oxide nanoparticles of nonstoichiometric composition and their high activity can readily be understood.

Thus, analysis of the Mössbauer spectra of the two iron-containing catalysts (2.5% Fe/AGM and 2.5% Fe/ASM) measured at temperatures from 3 to 300 K before and after 3,4-DCB isomerization shows that during the reaction some Fe^{III} ions in the γ-Fe_2O_3 nanoclusters magnetically ordered at 6 K and ~2—3 nm in size are reduced to the high-spin Fe^{II} complex in the paramagnetic state. According to the macroscopic magnetization data (SQUID), the initial clusters, on the one hand, demonstrate curves with hysteresis in the plots of forward and backward magnetization at 2 K. On the other hand, after the reaction completion this plot obtained at 2 K for the 2.5% Fe/ASM catalyst exhibits the linear field dependence of the magnetization passing through the coordinate origin. Analysis of the Mössbauer spectra and magnetic properties suggests that during the reaction the Fe^{III} ions in the γ-ferric oxide nanoclusters are partially reduced by the reaction medium to form the Fe^{II} complexes in which the chloride anions and O^{II} ion(s) of the silicate matrix serve as ligands. The formation of mixed-valence states of iron and insertion of the chloride anion

into the catalyst active phase cause, probably, the high activity of the γ-ferric oxide nanoparticles of nonstoichiometric composition in conversions of chloroolefins.

The authors are grateful to A. O. Chizhov for GC-MS analysis.

This work was financially supported by the Russian Foundation for Basic Research (Project No. 06-03-32006).

References

1. T. N. Rostovshchikova, M. S. Korobov, D. A. Pankratov, G. Yu. Yurkov, and S. P. Gubin, *Izv. Akad. Nauk*, *Ser. Khim.*, 2005, 1383 [*Russ. Chem. Bull., Int. Ed.*, 2005, **54**, 1425].
2. T. N. Rostovshchikova, V. V. Smirnov, M. V. Tsodikov, O. V. Bukhtenko, Yu. V. Maksimov, O. I. Kiseleva, and D. A. Pankratov, *Izv. Akad. Nauk*, *Ser. Khim.*, 2005, 1376 [*Russ. Chem. Bull., Int. Ed.*, 2005, **54**, 1418].
3. M. V. Tsodikov, T. N. Rostovshchikova, V. V. Smirnov, O. I. Kiseleva, Yu. V. Maksimov, I. P. Suzdalev, and V. N. Ikorskii, *Catal. Today*, 2005, **105**, 634.
4. T. N. Rostovshchikova, O. I. Kiseleva, G. Yu. Yurkov, S. P. Gubin, D. A. Pankratov, Yu. D. Perfil´ev, V. V. Smirnov, P. A. Chernavskii, and G. V. Pankina, *Vestn. MGU, Ser. 2. Khim.*, 2001, **42**, 318 [*Vestn. Mosk. Univ., Ser. Khim.*, 2001, **42** (Engl. Transl.)].
5. M. V. Tsodikov, Ya. R. Katsobashvili, E. V. Slivinskii, Yu. V. Maksimov, V. V. Matveev, I. P. Suzdalev, O. G. Ellert, and G. F. Ivanova, *Izv. Akad. Nauk SSSR*, *Ser. Khim.*, 1986, 2666 [*Bull. Acad. Sci. USSR, Div. Chem. Sci.*, 1986, **35**, 2443 (Engl. Transl.)].
6. Yu. V. Maksimov, M. V. Tsodikov, M. A. Perederii, I. P. Suzdalev, A. I. Nekhaev, V. T. Popov, and O. V. Bukhtenko, *Izv. Akad. Nauk*, *Ser. Khim.*, 1997, 86 [*Russ. Chem. Bull.*, 1997, **46**, 81 (Engl. Transl.)].
7. Yu. V. Maksimov, I. P. Suzdalev, V. N. Ikorskii, O. G. Ellert, V. M. Novotortsev, M. V. Tsodikov, and Kh. A. Navio, *Neorg. Mater.*, 2006, **42**, 1 [*Inorg. Mater.*, 2006, **42** (Engl. Transl.)].
8. L. A. Kazitsina and N. B. Kupletskaya, *Primenenie UF-, IK- i YaMR-spektroskopii v organicheskoi khimii* [*The Use of UV, IR, and NMR Spectroscopy in Organic Chemistry*], Vysshaya Shkola, Moscow, 1971, 236 (in Russian).
9. B. V. Kuznetsov, S. N. Lanin, T. A. Rakhmanova, V. V. Smirnov, M. V. Tsodikov, and D. V. Tarasova, *Zh. Fiz. Khim.*, 2007, **81**, No. 5 [*Russ. J. Phys. Chem.*, 2007, **81** (Engl. Transl.)].
10. S. V. Vonsovskii, *Magnetizm* [*Magnetism*], Nauka, Moscow, 1984, 112 (in Russian).
11. G. S. Kandaurova and L. T. Onoprienko, *Domennaya struktura magnetikov. Osnovnye voprosy mikromagnetiki* [*Domain Structure of Magnetics. The Main Problems of Micromagnetics*], Izd-vo UrGU, 1986, 106 (in Russian).
12. N. N. Greenwood and T. C. Gibb, *Mössbauer Spectroscopy*, Chapman and Hall, London, 1971, 117.
13. E. Pfletschinger, *Z. Physik.*, 1968, **200**, 119.
14. S. Chandra and G. R. Hoy, *Phys. Lett.*, 1966, **22**, 254.
15. F. Alonso, I. P. Beletskaya, and M. Yus, *Chem. Rev.*, 2002, **102**, 4009.
16. O. V. Krylov, *Geterogennyi kataliz* [*Heterogeneous Catalysis*], Akademkniga, Moscow, 2004, 337 (in Russian).

Received May 18, 2006;
in revised form September 13, 2006